

Electronic Supplementary Information:

Cluster-model DFT simulations of the infrared spectra of triazine-based molecular crystals

Xiaohong Yuan,^a Kun Luo,^{ab} Nan Liu,^a Xueqiang Ji,^a Chao Liu,^a Julong He,^a Guangjun Tian,^b
Yuanchun Zhao^{*a} and Dongli Yu^{*a}

^aState Key Laboratory of Metastable Materials Science and Technology, Yanshan University,
Qinhuangdao 066004, China.

^bHebei Key Laboratory of Microstructural Material Physics, School of Science, Yanshan University,
Qinhuangdao 066004, China

*E-mail: yzhao56@ysu.edu.cn (Y.C.Z.); ydl@ysu.edu.cn (D.L.Y.)

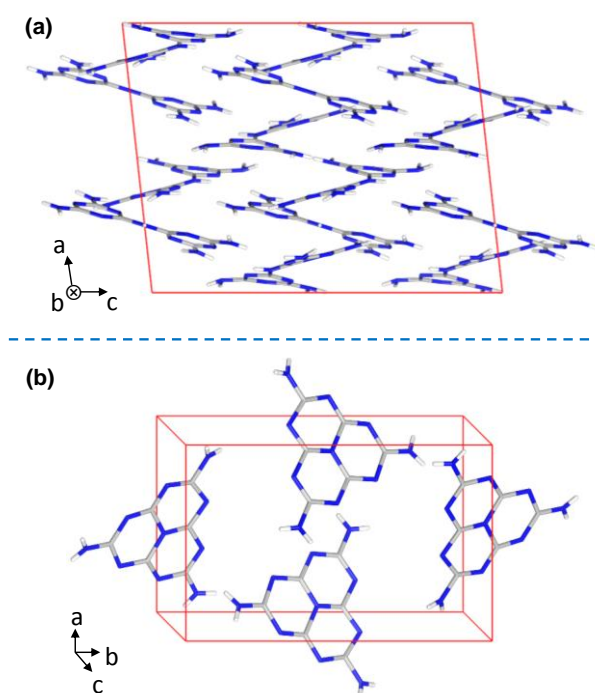


Fig. S1 Crystal structures of (a) melam reported by Lotsch and Schnick in ref. S1 (lattice parameters: $C2/c$, $a = 18.11 \text{ \AA}$, $b = 10.87 \text{ \AA}$, $c = 13.98 \text{ \AA}$, and $\beta = 96.31^\circ$) and (b) melem reported by Jürgens et al. in ref. S2 (lattice parameters: $P2_1/c$, $a = 7.40 \text{ \AA}$, $b = 8.65 \text{ \AA}$, $c = 13.38 \text{ \AA}$, and $\beta = 99.91^\circ$). The C, N, and H atoms are distinguished with dark grey, blue, and light grey colors, respectively.

Note: The crystal structure and X-ray diffraction pattern of melamine can be found in our previous work.^{S3}

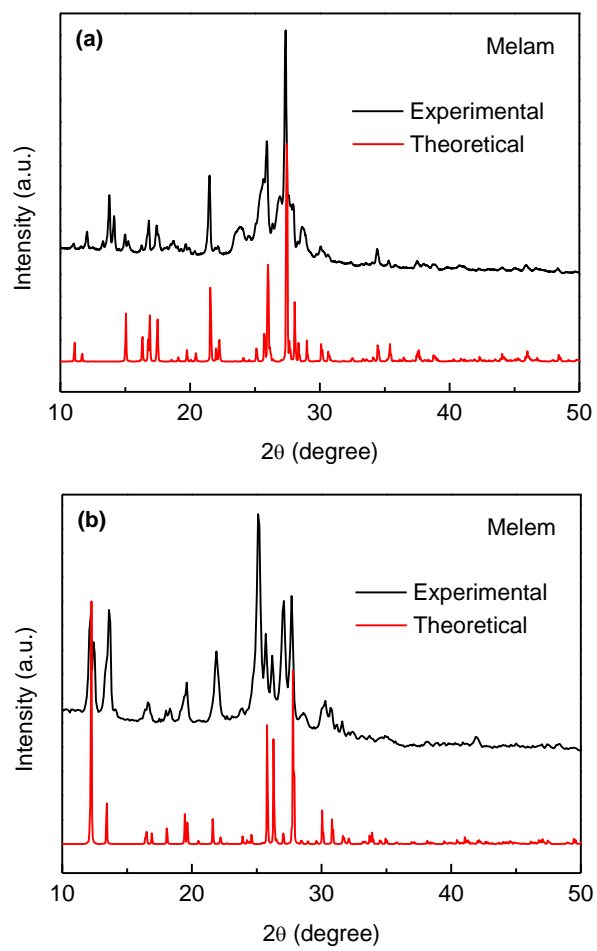


Fig. S2 Experimental and theoretically generated XRD patterns of (a) melam, and (b) melem.

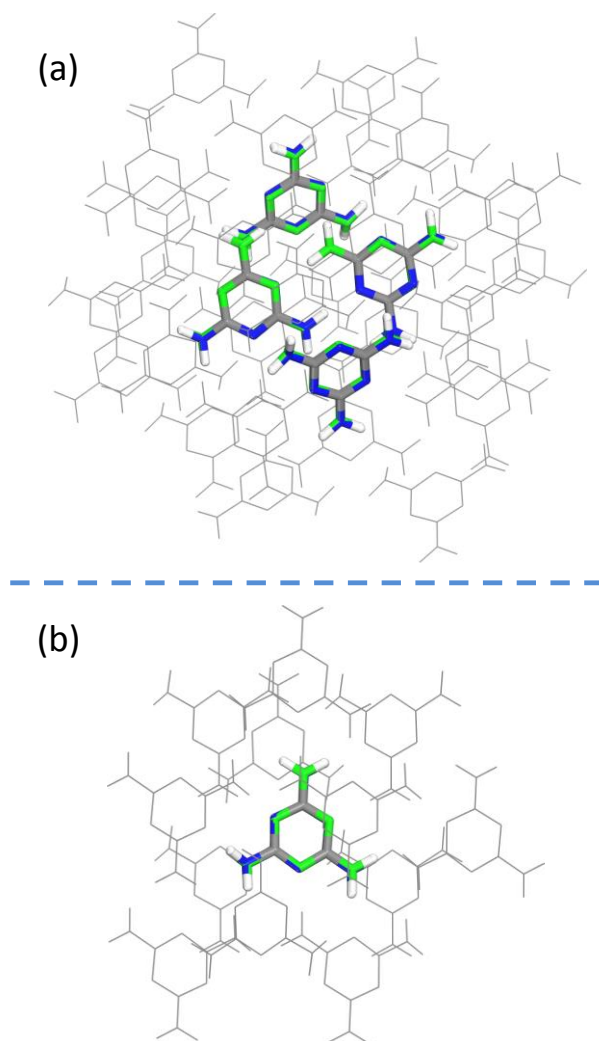


Fig. S3 Comparison between molecular geometries before and after geometry optimization of (a) the 32-molecule cluster, and (b) the 13-molecule cluster of melamine. The **blue(N)**-grey(C)-white(H) colored structures represent the models directly extracted from **the crystal structure of melamine**, and the **green(N)**-grey(C)-white(H) colored structures are those **optimized by Gaussian 16 software package** for further IR calculations.

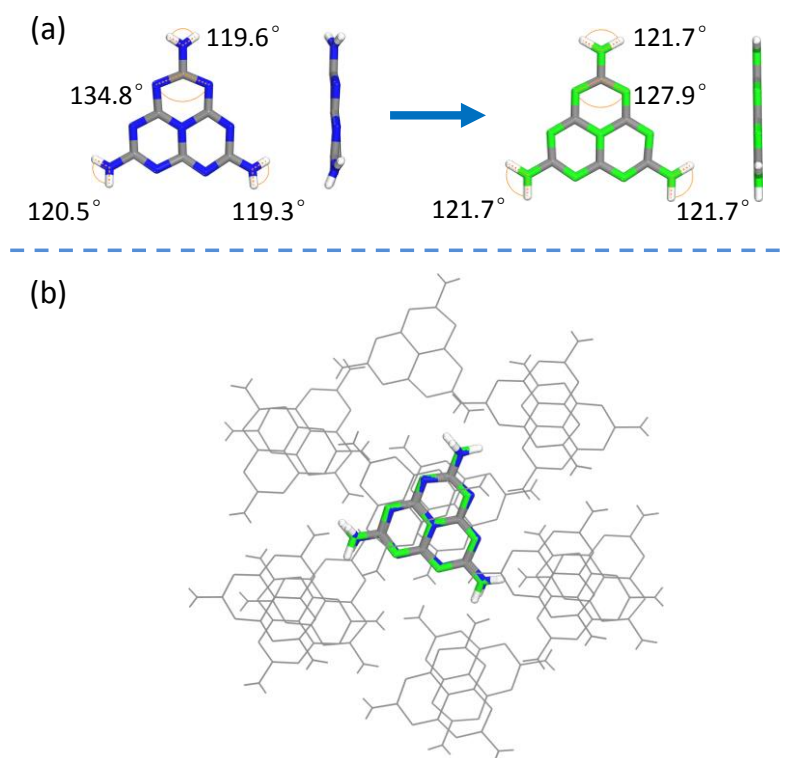


Fig. S4 Comparison between molecular geometries before and after geometry optimization of (a) a single molecule, and (b) the built 16-molecule cluster of melem. The **blue(N)**-grey(C)-white(H) colored structures represent the models directly extracted from **the crystal structure of melem**, and the **green(N)**-grey(C)-white(H) colored structures are those **optimized by Gaussian 16 software package** for further IR calculations.

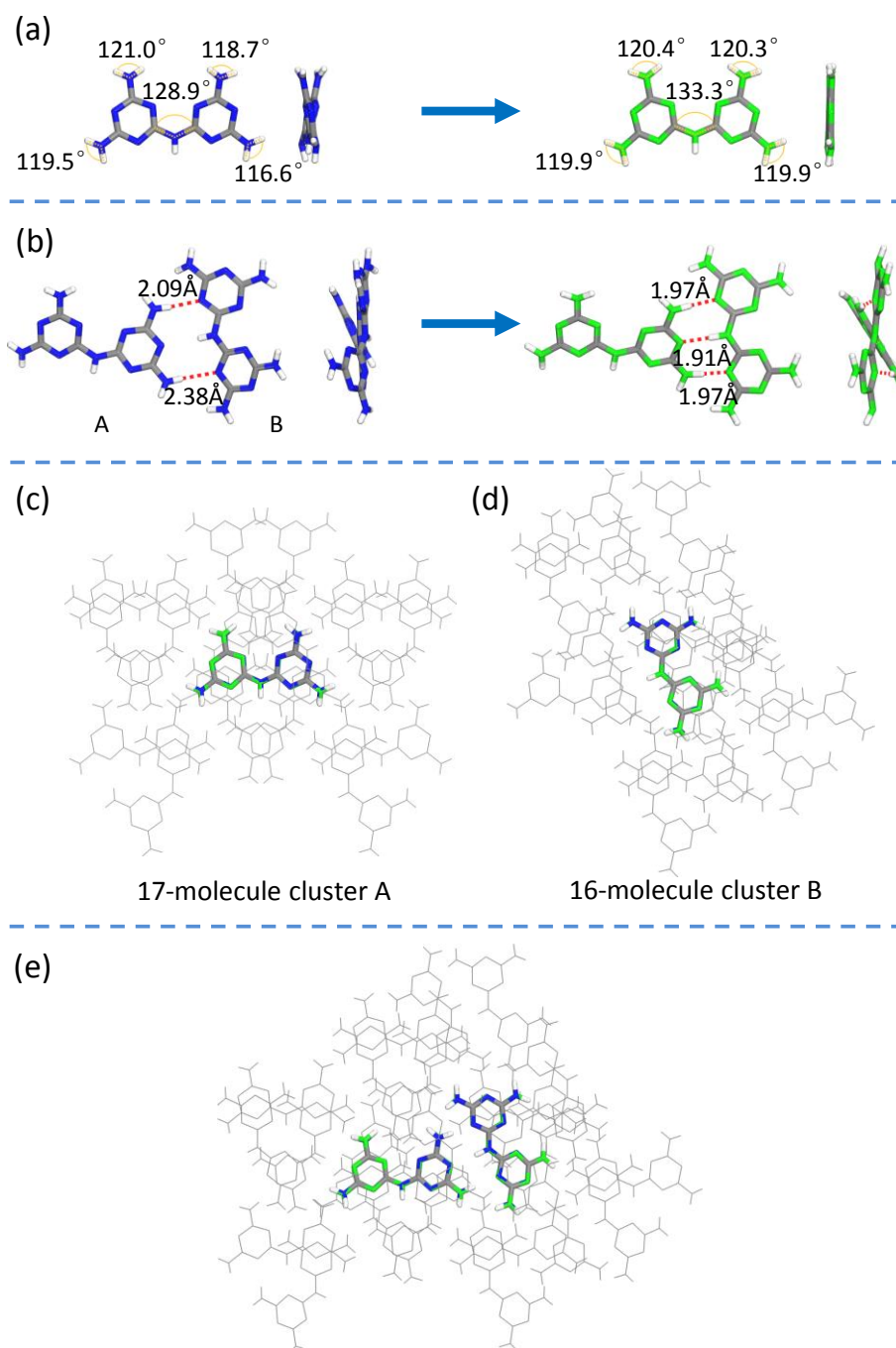


Fig. S5 Comparison between molecular geometries before and after geometry optimization of (a) a single molecule and (b) the 2-molecule cluster, (c) the 17-molecule cluster A, (d) the 16-molecule cluster B, and (e) the finally built 25-molecule cluster of melam. The **blue(N)**-grey(C)-white(H) colored structures represent the models directly extracted from **the crystal structure of melam**, and the **green(N)**-grey(C)-white(H) colored structures are those **optimized by Gaussian 16 software package** for further IR calculations.

Table S1 Details of the molecules and cluster models designed for IR calculations in this work, which were directly extracted from the corresponding crystal structures and the geometry optimizations were performed by the Gaussian 16 software package.

	models	total atom numbers	Representative molecules	numbers of the surrounding molecules hydrogen-bonded with the representative ones	numbers of the formed hydrogen bonds with the representative molecules	computational costs ^a
melamine	32-molecule cluster	480	4	12	30	31 h
	13-molecule cluster	195	1	4	8	4.5 h
melem	single molecule	22	1	0	0	0.5 h
	16-molecule cluster	352	1	5	8	12.2 h
melam	single molecule	26	1	0	0	0.6 h
	2-molecule cluster	52	2	0	from 2 to 3 (before and after geometry optimization)	3 h
	17-molecule cluster A	442	1	6	10	24 h
	16-molecule cluster B	416	1	6	11	19 h
	25-molecule cluster	650	2	10	19	65.5 h

^aComputer server: Super Sever X10QBL-4, 4 x 2.10 GHz Xeon[®] Processor E7-8870 v3/18 Core, 16 x 16 GB ECC DDR3/2133 MHz; the single-molecule models (melem and melam) and the 2-molecule model of melam were calculated using 20 cores with a memory of 45 GB; the rest of 6 cluster models were calculated using 60 cores with a memory of 230 GB.

Note: As summarized in Table S1, totally 9 models have been designed for the IR simulations in this work. By considering the crystallographic equivalence of the corresponding crystal structures, only one representative molecule has been determined for melamine and melem, respectively; while for melam two crystallographically independent molecules need to be considered. We have further built specific cluster models based on the two different molecules of melam A and B (Fig. S5), which present different molecule numbers as well as distinct hydrogen-bonding environments. For the 2-molecule cluster of melam, two hydrogen bonds are formed between the considered molecules, whereas after geometry optimization an additional hydrogen bond is formed with the bridging N–H bond of melam B (Fig. S5b). The computational costs of all the listed models have also been combined into Table S1 as a reference.

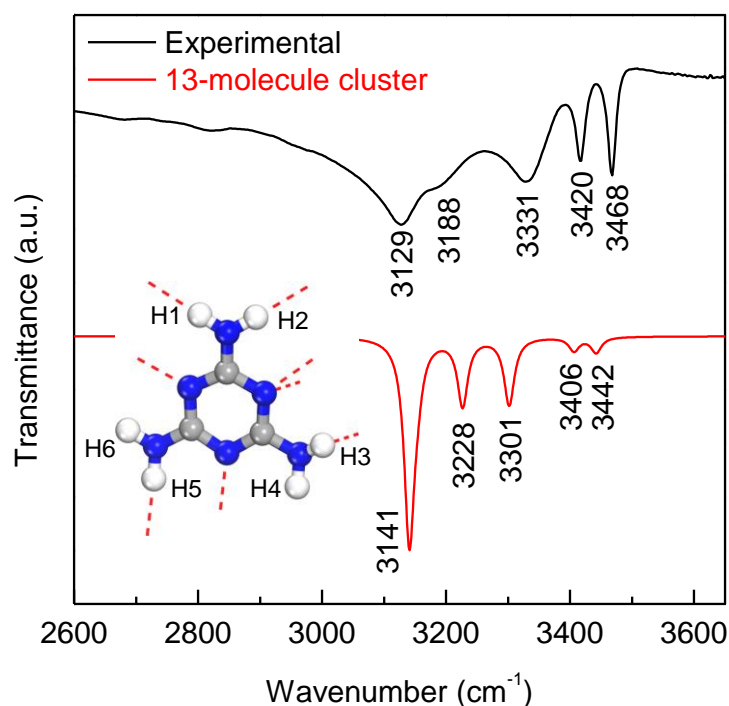


Fig. S6 Zoomed FTIR spectra of melamine showing the characteristic NH_2 stretching region. The inset shows the representative molecule and the formed hydrogen bonds, N-H4 and N-H6 are free from hydrogen bonding and thus show remarkably small intensities at 3406 and 3442 cm^{-1} in the simulated spectra.

Table S2 Comparison between the experimental IR absorption peaks and those in the stimulated 13-molecule-cluster spectrum of melamine related to the characteristic NH_2 stretching modes. The dominant components of each vibration mode have been highlighted, respectively.

wavenumber (cm^{-1})		assignments ^a	detailed vibrational components ^b
experimental	calculated		
3129	3141	ν_s	NH1(m)+NH2(s)+NH3(w)+NH4(w)+NH5(s)+NH6(m)
3188	3228	ν_s	NH1(w)+NH2(w)+NH3(s)+NH4(m)+NH5(w)+NH6(w)
3331	3301	ν_{as}	NH1(s)+NH2(s)
3420	3406	ν_{as}	NH3(m)+NH4(s)
3468	3442	ν_{as}	NH5(m)+NH6(s)

^a ν_s : symmetrical stretching vibration, ν_{as} : asymmetrical stretching vibration. ^bs: strong, m: medium, w: weak.

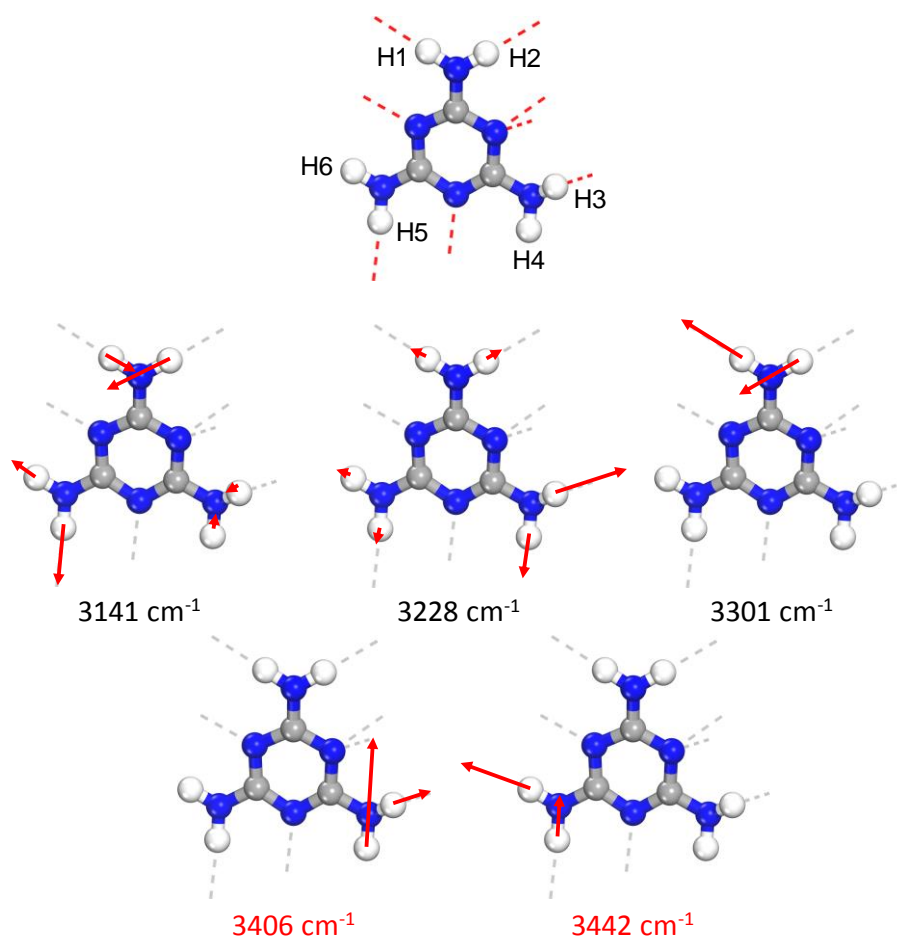


Fig. S7 Calculated eigenvectors of the characteristic NH_2 stretching modes of melamine at 3141, 3228, 3301, 3406 and 3442 cm^{-1} . The latter two modes are dominated by the stretching vibrations of N–H4 and N–H6 bonds, which are free from hydrogen bonding. The C, N and H atoms are distinguished by dark grey, blue, and light grey colors, respectively.

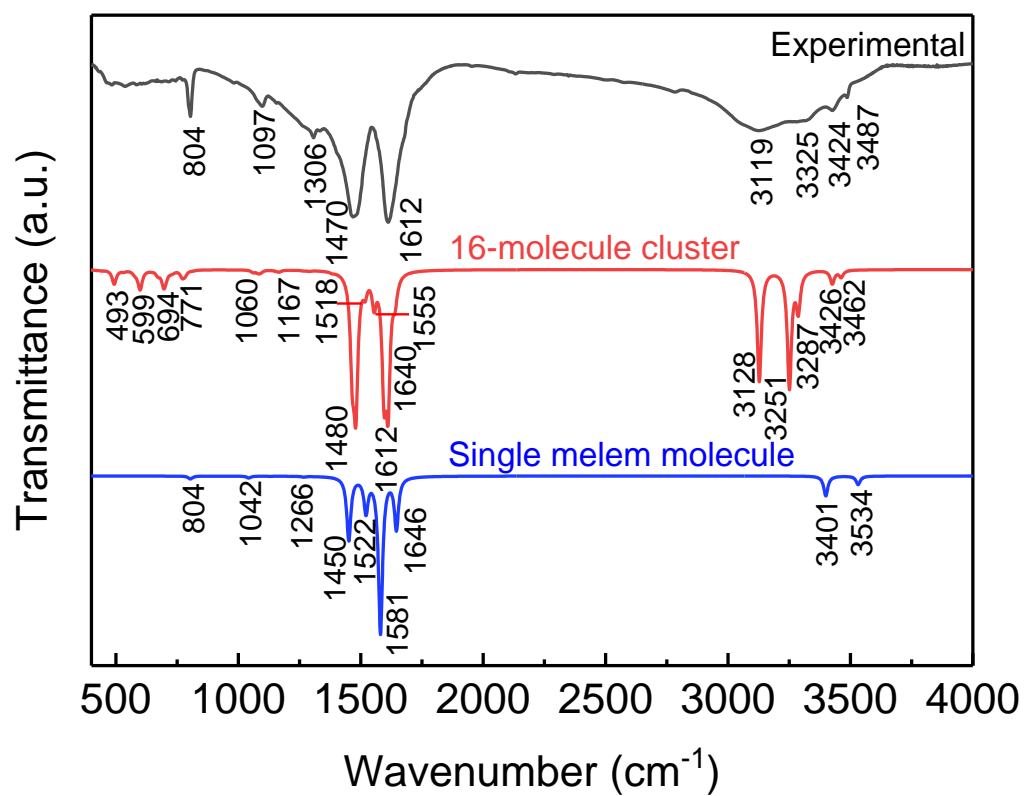


Fig. S8 Detailed IR peak positions in the experimental and simulated spectra of melem based on different models.

Table S3 Comparison between the experimental IR absorption peaks and the calculated wavenumbers of melem based on a single molecule and the built 16-molecule cluster and the corresponding combinatorial vibration-mode assignments.

calculated			experimental	
wavenumbers (cm ⁻¹)		combinatorial vibration-mode assignments ^a	wavenumbers (cm ⁻¹)	assignments ^{S2}
single melem molecule	16-melem cluster			
	493,599,694	$\gamma(\text{NH})$	478,597,740 ^b	
804	771	$\gamma(\text{CN}) + \gamma(\text{NH})$	804	the ring-sextant out-of-plane bending
1042	1060,1090	$\rho(\text{NH}_2) + \nu(\text{CN})$	1097	NH stretching
1266	1167	$\rho(\text{NH}_2) + \nu(\text{CN1})^c$		
			1306	CNC bending
1450	1465,1480	$\rho(\text{NH}_2) + \delta(\text{NH}_2) + \nu(\text{CN})$	1470	side-chain CN breathing
1521	1518	$\delta(\text{NH}_2) + \nu(\text{CN})^{\text{OR}} + \nu(\text{CN4,5})$		
1580	1555	Ring breathing + $\delta(\text{NH}_2)$		
1645	1595,1612,1640	$\nu(\text{CN2-7}) + \delta(\text{NH}_2)$	1612	NH ₂ bending
3401	3128	$\nu_s(\text{N8H}_2)$	3119	
	3251	$\nu_{\text{as}}(\text{N8H}_2) + \nu_s(\text{N9H}_2)$	3325	
				NH stretching
3534	3287,3426,3462	$\nu_{\text{as}}(\text{NH}_2)$	3424,3487	

^a ν_s : symmetrical stretching vibration, ν_{as} : asymmetrical stretching vibration, ν : stretching vibration, β : in-plane bending vibration, δ : shearing vibration, ρ : in-plane rocking vibration, γ : out-of-plane bending vibration, R: mode on the ring atoms, OR: mode out of the ring.

^bThese three peaks are observed in the experimental spectrum in ref. S2 but absent from the spectrum in this study. ^cN atoms are numbered in the top panel of Fig. S9.

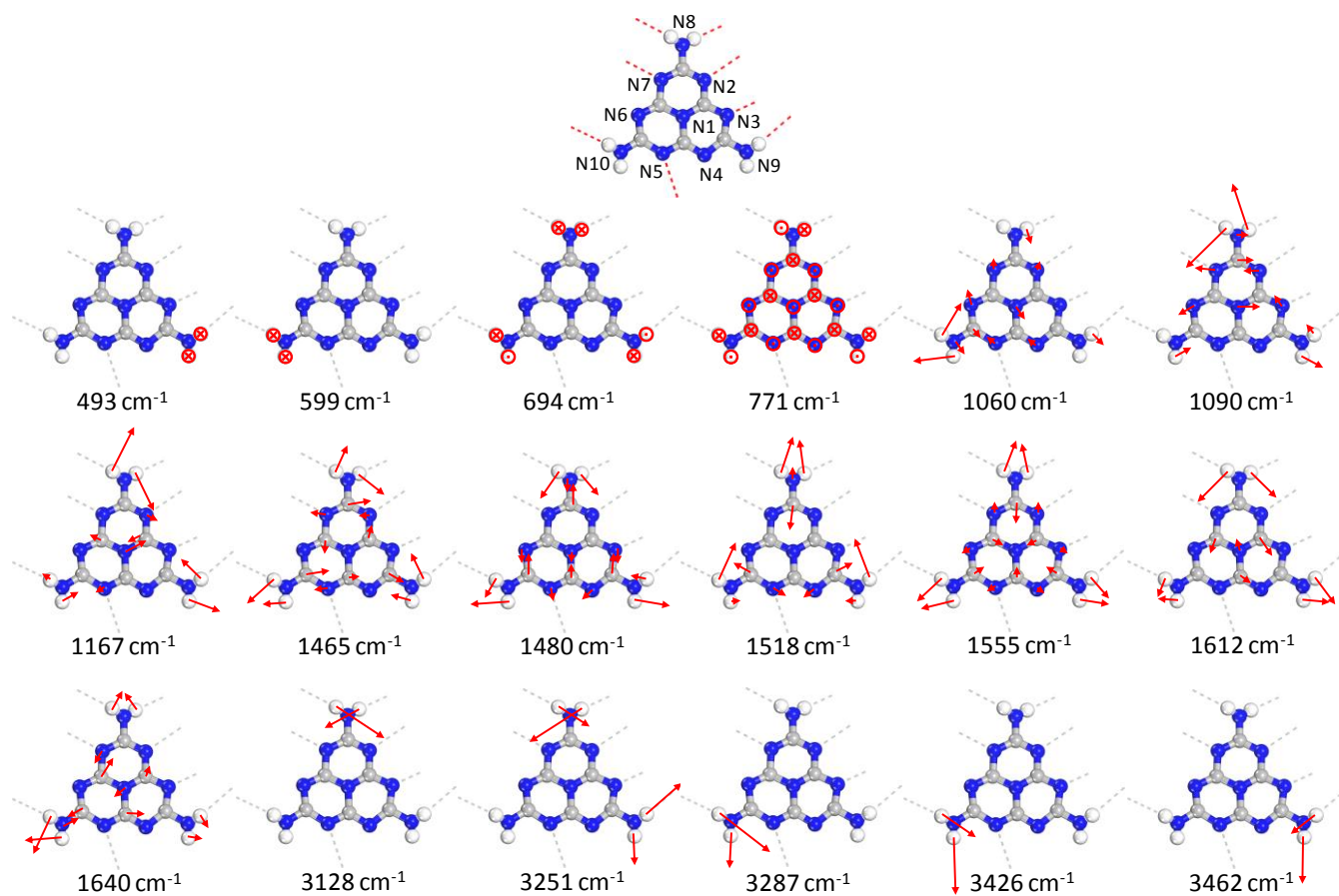


Fig. S9 Calculated eigenvectors of the characteristic vibrational modes of melem based on the built 16-molecule cluster. The C, N and H atoms are distinguished by dark grey, blue, and light grey colors, respectively.

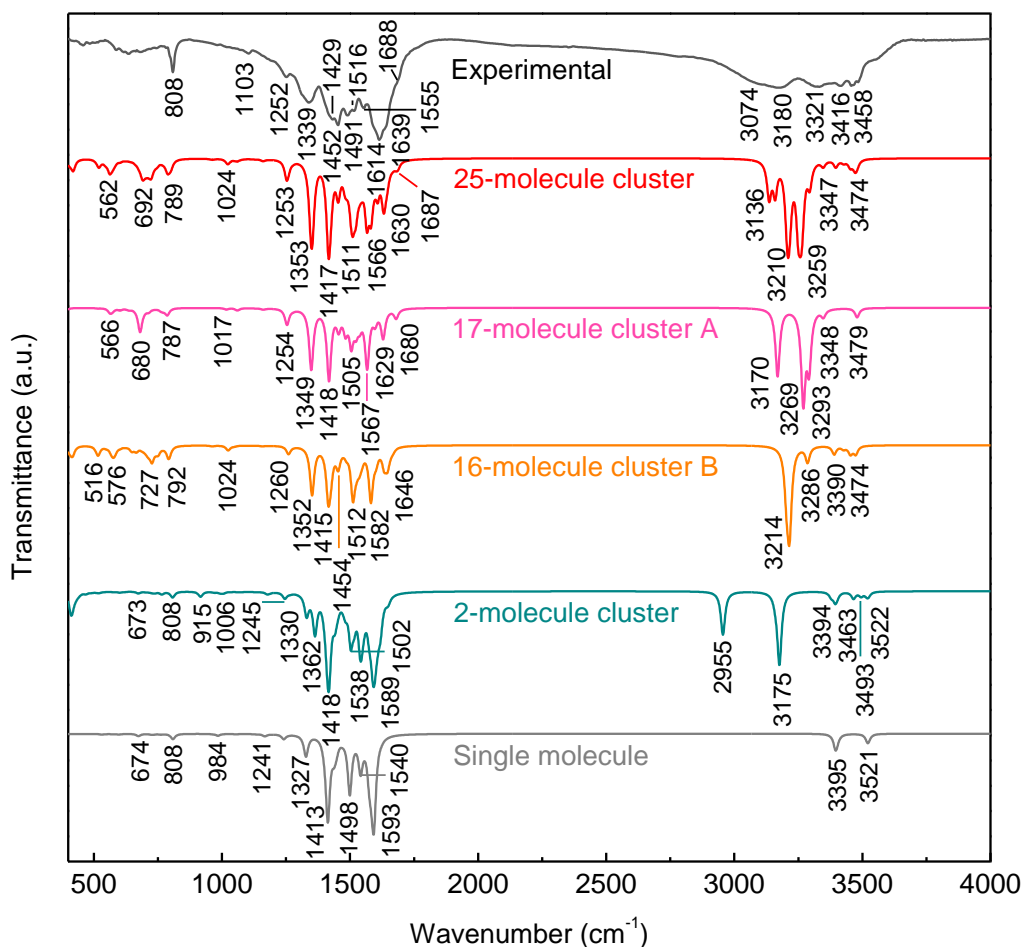


Fig. S10 Detailed IR peak positions in the experimental and simulated spectra of melam based on different models.

Note: The absorption bands in range of $1200\text{--}1700\text{ cm}^{-1}$ correspond to the vibrational modes of C–N/C=N stretching and NH/NH₂ shearing. As shown in Fig. S10, the peaks at 1253, 1353, 1417, and 1566 cm^{-1} observed in the 25-molecule-cluster spectrum are dominated by the intramolecular C–N/C=N stretching (Table S5 and Fig. S11), and the corresponding peaks can be identified in other simulated spectra, even the one based on a single molecule. However, the vibrational peaks at 1454, 1511, 1630, and 1687 cm^{-1} in the 25-molecule-cluster spectrum are mainly related to the NH/NH₂ shearing and NH in-plane rocking, significant differences have been observed in other simulated spectra including those based on the 17-molecule cluster with melam A and 16-molecule cluster with melam B, indicating these vibrational modes are more sensitive to the surrounding crystallographic environments.

Table S4 Comparison of the experimental IR absorption peaks and the calculated wavenumbers of melam based on different models.

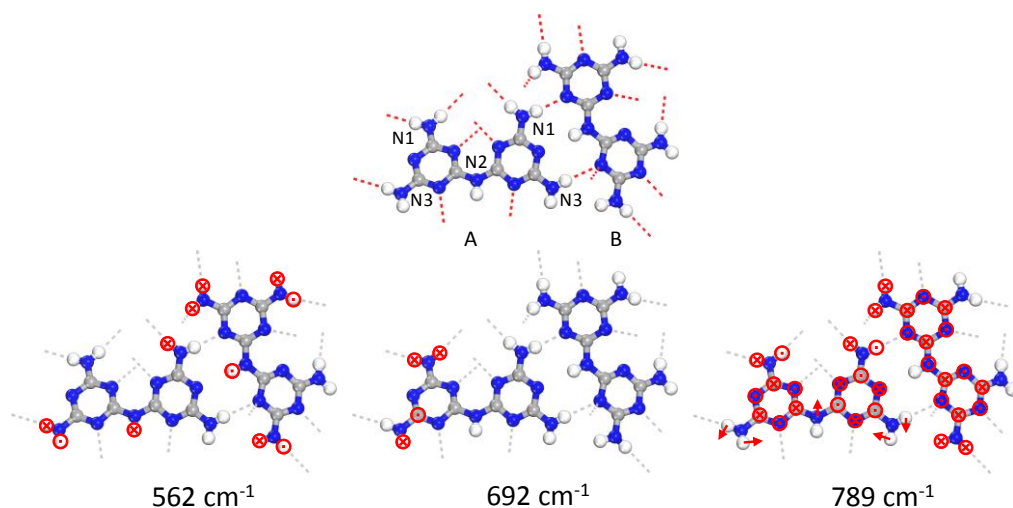
experimental absorption peak (cm ⁻¹)	calculated wavenumbers (cm ⁻¹)				
	25-molecule cluster	17-molecule cluster A	16-molecule cluster B	2-molecule cluster	single molecule
	562,692	566, 680	516, 576, 727,751	673	674
808	789	787	792	808	808
1103	1024,1060	1017	1024	915,1006	984
1252	1253	1254	1260	1245	1241
1339	1353	1349	1352	1330, 1362	1327
1429	1417	1418	1415	1418	1413
1452	1454	1456	1454	1442	1439
1491,1516	1511	1505	1512	1502,1538	1498,1540
1555	1566	1567	1582	1589	1593
1614	1608	1598	1601	1617	
1639	1630	1629	1646	1649	
1688	1687	1680		2955	
3074	3136,3159				
3180	3210	3170	3214	3175	
	3259	3269			3395
3321	3294	3293	3286		
	3347	3348			
3416	3396,3427		3390,3426	3394,3463	
3458	3453,3474	3479	3454,3474	3493,3522	3521

Table S5 Comparison between the experimental IR absorption peaks and calculated wavenumbers of melam based on the finally built 25-molecule cluster and the corresponding combinatorial vibration-mode assignments.

calculated (25-molecule cluster)		experimental	
wavenumbers (cm ⁻¹)	combinatorial vibration-mode assignments ^a	wavenumbers (cm ⁻¹)	assignment ^{S1,S4}
562,692	$\gamma(\text{NH})$		
789	$\gamma(\text{CN}) + \gamma(\text{NH})$	808	the characteristic sextant ring bending
1024 (molecule B)	$\rho(\text{N2H})^b$		
1060 (molecule A)			
1253	$\rho(\text{NH}) + \nu(\text{CN})^{\text{R}}$	1252	
1353	$\rho(\text{NH}) + \nu(\text{CN})^{\text{OR}}$	1339	
1417	$\delta(\text{NH}) + \nu(\text{CN})^{\text{OR}}$	1429	
1454	$\delta(\text{NH}) + \nu(\text{CN})^{\text{OR}} + \beta(\text{CN2C})$	1452	C–N/C=N stretching and NH/NH2 shearing
1511	$\delta(\text{NH}) + \beta(\text{CNH})$	1491,1516	
1566	$\delta(\text{N1H}) + \rho(\text{N3H}) + \nu(\text{CN})^{\text{R}}$	1555	
1608	$\rho(\text{NH})$	1614	
1630,1687			
3136,3159,3210	$\nu_{\text{s}}(\text{NH}_2)$	3074,3180	
3249,3259	$\nu_{\text{as}}(\text{NH}_2) + \nu(\text{N2H})$	3321	
3294	$\nu_{\text{s}}(\text{NH}_2)$		characteristic N–H stretching
3347	$\nu(\text{N2H})$	3416	
3396,3427	$\nu_{\text{as}}(\text{NH}_2)$	3458	
3453,3474		3562	

^a ν_{s} : symmetrical stretching vibration, ν_{as} : asymmetrical stretching vibration, ν : stretching vibration, β : in-plane bending vibration, δ : shearing vibration, ρ : in-plane rocking vibration, γ : out-of-plane bending vibration, R: mode on the ring atoms, OR: mode out of the ring.

^bN atoms are numbered in the top panel of Fig. S11.



(to be continued)

(continued)

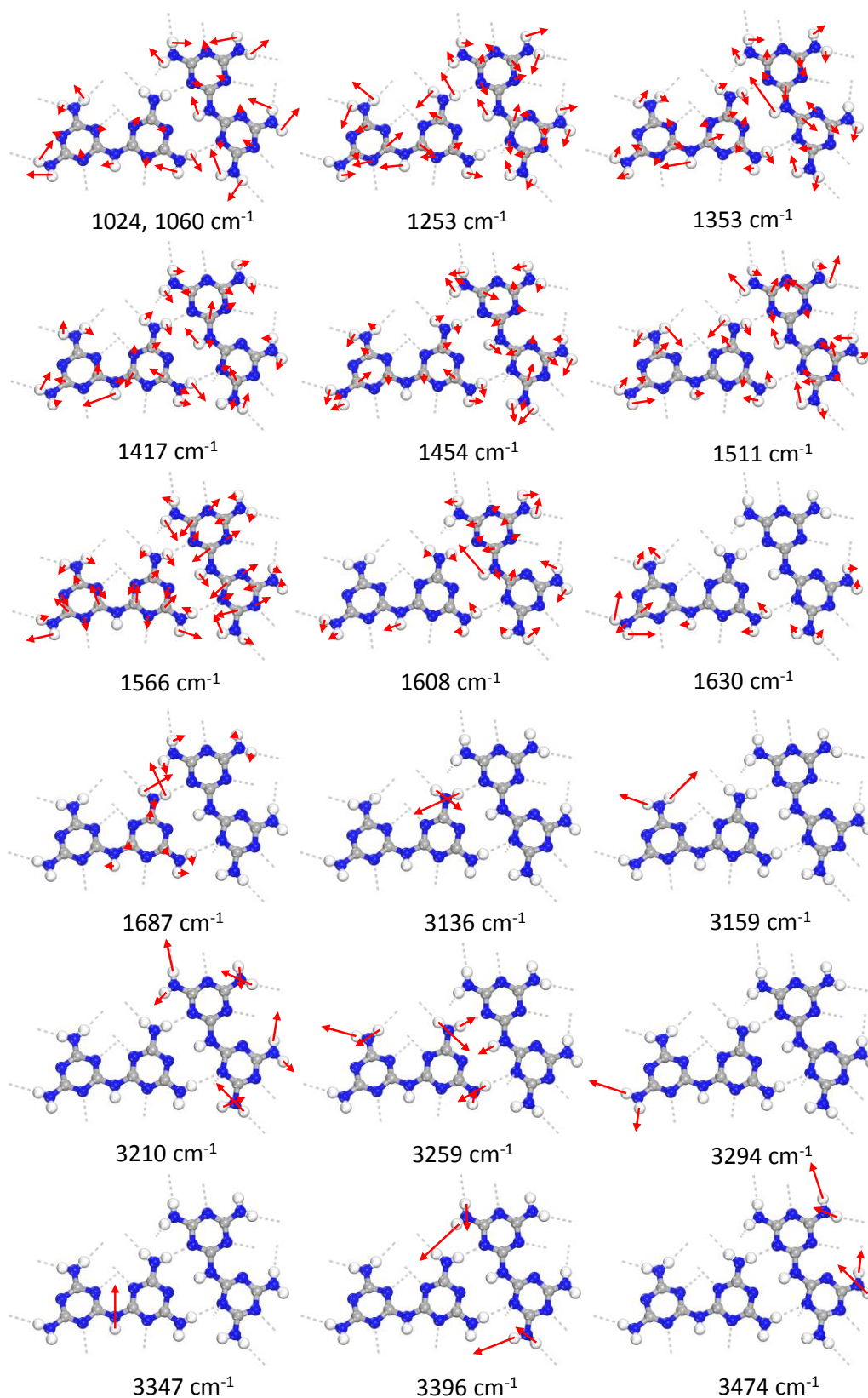


Fig. S11 Calculated eigenvectors of the characteristic vibrational modes of melam based on the finally built 25-molecule cluster. The C, N and H atoms are distinguished by dark grey, blue, and light grey colors, respectively.

References

- S1 B. V. Lotsch and W. Schnick, *Chem. Eur. J.*, 2007, **13**, 4956–4968.
- S2 B. Jürgens, E. Irran, J. Senker, P. Kroll, H. Müller and W. Schnick, *J. Am. Chem. Soc.*, 2003, **125**, 10288–10300.
- S3 X. Yuan, K. Luo, K. Zhang, J. He, Y. Zhao and D. Yu, *J. Phys. Chem. A*, 2016, **120**, 7427–7433.
- S4 E. Wirnhier, M. B. Mesch, J. Senker and W. Schnick, *Chem. Eur. J.*, 2013, **19**, 2041–2049.